SYNTHESIS OF ASYMMETRICALLY SUBSTITUTED SCYLLO-INOSITOL

by

Jacob Joshua Lee Rodriguez

Department of Chemistry and Biochemistry

University of Colorado at Boulder

2018

Advisor: Maciej Walczak, Department of Chemistry and Biochemistry

Committee:

Maciej Walczak, Department of Chemistry and Biochemistry

Robert Parson, Department of Chemistry and Biochemistry

Bradley Olwin, Department of Molecular, Cellular, and Developmental Biology

Defended on April 5 2018

TABLE OF CONTENTS

LIST OF FIGURES

LIST OF SCHEMES

LIST OF ABBREVIATIONS

a.u.: Atomic Unit

Ac: Acetyl

Acac: Acetylacetonate

An: Acrylonitrile

Ar: Aromatic ring

Bn: Benzyl

Boc: tert-Butoxycarbonyl

n-Bu: n-Butyl

t-Bu: tert-Butyl

Bz: Benzoyl

Cod: 1,5-Cyclooctadiene

COE: Cyclooctene

Cp: Cyclopentadienyl

Cy: Cyclohexyl

DBU: 1,8-Diazabicyclo[5.4.0]undec-7-ene

DEAD: Diethyl azodicarboxylate

DHP: 3,4-Dihydro-2H-pyran

DIAD: Diisopropyl azodicarboxylate

DIPEA: N,N-Diisopropylethylamine

DMAD: Dimethyl Acetylenedicarboxylate

DME: Dimethoxyethane

DMF: N,N-Dimethylformamide

DMS: Dimethyl sulfide

Dppb: 1,4-Bis(diphenylphosphino)butane

dppb: 1,3-Bis(diphenylphosphino)propane

dppe: 1,2-Bis(diphenylphosphino)ethane

dppm: Bis(diphenylphosphino)methane

Et: Ethyl

EWG: Electron-withdrawing group

HOMO: Highest Occupied Molecular Orbital

LG: Leaving group

LUMO: Highest Occupied Molecular Orbital

Me: Methyl

MNP: 2-Methyl-2-nitrosopropane

Ms: Methanesulfonyl

MS: Mass Spectrometry

MS-TOF: Time-of-Flight Mass Spectrometry

μW: Microwave irradiation

ND: Not determined

NMO: N-Methylmorpholine-N-oxide

NMR: Nuclear Magnetic Resonance Spectroscopy

P.E.: Petroleum ether

PCC: Pyridinium chlorochromate

PDC: Pyridinium dichromate

Ph: Phenyl

i-Pr: i-Propyl

n-Pr: n-Propyl

PPTS: Pyridinium 4-toluenesulfonate

RT: Room temperature

SES: 2-(Trimethylsilyl)ethanesulfonyl

TBAF: Tetra-n-butylammonium fluoride

TBDPS: tert-Butyldiphenylsilyl

TBS: tert-Butyldimethylsilyl

Tf: Trifluoromethanesulfonyl

TFA: Trifluoroacetic acid

TIPS: Triisopropylsilyl

TMEDA: Tetramethylethylenediamine

TMS: Trimethylsilyl

Tol: 4-Methylphenyl

TPAP: Tetra-n-propylammonium perruthenate

Tris: 2,4,6-Triisopropylbenzenesulfonyl

Ts: 4-Toluenesulfonyl

TSA: 4-Toluenesulfonic acid

ACKNOWLEDGMENTS

I would like to thank Prof. Maciej Walczak for his continued guidance and mentorship for all of my projects throughout my undergraduate experience. I cannot imagine where I would be now without his support.

I would like to thank the members of my lab who have always been available to talk about chemistry. A special thanks goes out to Dr. Feng Zhu who has guided me to become a more practical and effective chemist, and a special thanks goes out to Tianyi Yang who has continued to be by my side, aiding me as a mentor and friend, throughout my entire undergraduate career.

I would additionally like to thank my committee members Bradley Olwin and Robert Parson for taking time to support me in developing my thesis. I would also like to thank the Bob and Dickie Lacher fund, specifically Bob and Jan Lacher for making it possible for me to conduct research without financial worry. I would also like to thank Bob and Jan Lacher for their kindness and support.

1.0 SYNTHESIS OF AXINELLOSIDE A SEGMENTS

Although the microscopic world is opaque in its complexity and diversity, small and well-defined molecules grant access to reliably investigate and control otherwise elusive cellular processes. Molecules containing potent biological activity are excreted from a number of different types of uni- and multi-cellular organisms to communicate with and kill competing organisms. Axinelloside A **(1)**, a small molecule isolated from the marine sponge, *Axinella infundibula*, poses as one of these biological molecules with an inhibitory concentration (IC_{50}) of 0.4 μM for the enzyme telomerase, which is an enzyme important for the regulation of cancer.[1] Unfortunately, methods for obtaining axinelloside A from its natural source involve laborious, kilogram-scale extractions followed by more tedious isolation and purification to yield only a few milligrams of axinelloside A—hardly enough to modify and use for further investigation. Axinelloside A is a 12-member oligosaccharide comprised of multiple galactose and fucose sugars along with an arabinose and *scyllo*-inositol group. A convergent synthesis of these 12 parts offers an alternative pathway to access more substantial quantities of the molecule for exploration of its unique activity.

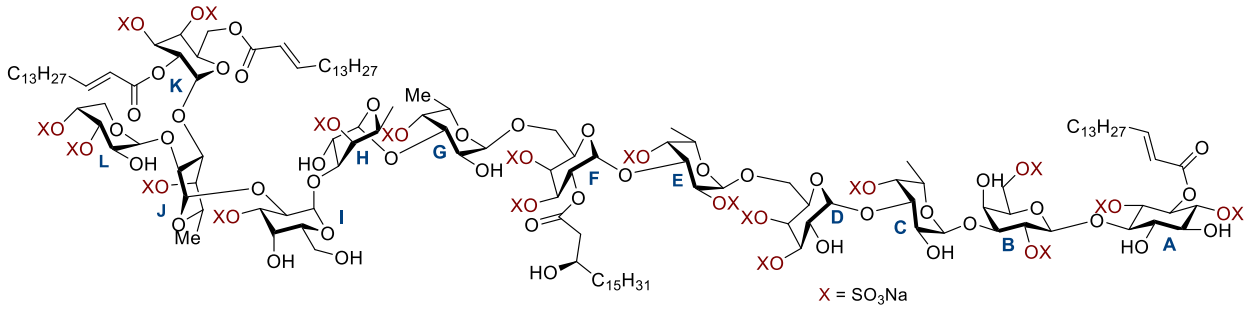

(1)

Figure 1: axinelloside A. Shown is the molecular structure for axinelloside A **(1)**. Each of the sugar residues that constitute the molecule is labelled (A-L), and sulfate moieties are colored red. Sodium is chosen as the sulfate counter ion.

1.1 INTRODUCTION

1.1.1 Axinelloside A

The isolation of small molecules from natural sources (natural products) has either directly generated or inspired the synthesis of a multitude of clinical drugs. [2] These compounds are typically isolated from terrestrial organisms, but increasing numbers of compounds isolated form marine organisms prove the ocean to be another viable source of useful natural products. A significant portion of marine life exists without an established immune system and must therefore defend itself from invading, proliferating cells through the excretion of unique natural products. Ever since an incentive to discover these marine natural products in 1990, a growing number of molecules have been isolated containing unique biological properties, notably, as anti-proliferative agents. [3]

While many anti-proliferative molecules kill cells, general cytotoxicity is hardly useful when considering therapeutic drugs. Molecules with highly promiscuous activity invariably fail to become clinical drugs because a general mode of action results in wide-spread cell death and deleterious side-effects *in vivo*. [4] Dozens of the isolated marine natural product molecules, however, specifically inhibit the enzyme telomerase. Dictyodendrins, Axinellosides, meridine, (figure 2), and many other sulfated polysaccharides and alkaloids have been isolated, each bearing a wide array of different functional groups, stereochemistry, conjugation, and reactive sites. [5] With IC_{50} values ranging from 50 µM to 0.4 µM, these molecules maintain anti-proliferative action *via* selective inhibition of an enzyme that significantly contributes to the endless replication of

cells. Of all these isolated marine natural products, Axinelloside A (figure 1) is recognized as the most potent inhibitor to human telomerase with and IC_{50} of 0.4 µM.

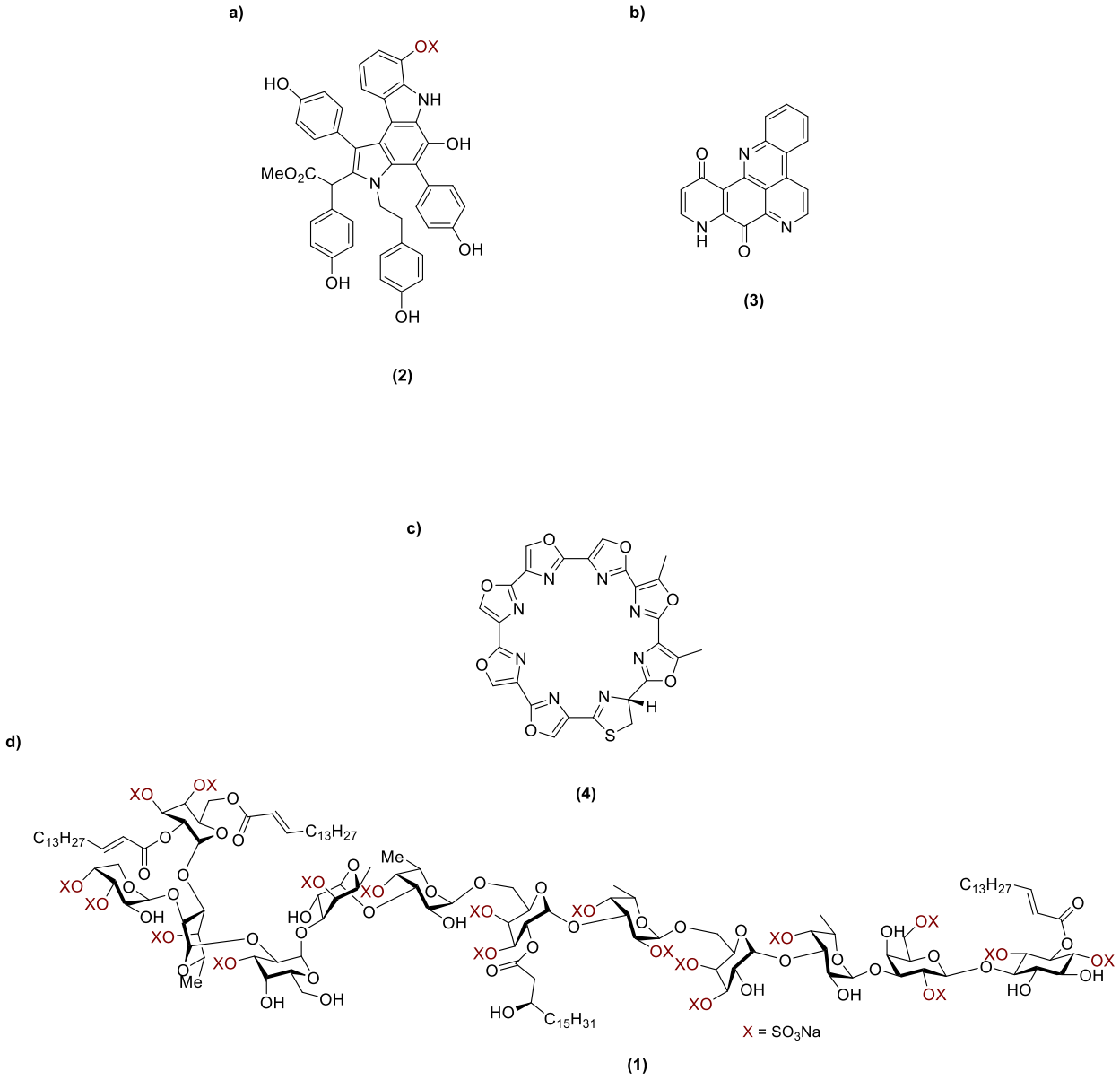

Figure 2: selected examples of marine natural products that inhibit telomerase. a) Dictryodentrin A, isolated from the sponge *Dictyodendrilla verongiformis*. [5b] b) Meridine, isolated from the ascidian *Amphicarpa meridiana*. [5a] c) Telomestatin, isolated from the bacteria *Streptomyces anulatus*. [6] d) Axinelloside A, isolated from the sponge *Axinella infundibula*. [1]

In order to understand the significance of axinelloside A, it is important to understand the activity of the enzyme it inhibits: telomerase. When cells replicate, enzymatic machinery duplicates cellular DNA using one strand of the original double helix as a template strand. Since the two strands that make up a DNA helix run antiparallel with respect to one another, synthesis of new strands takes two approaches. The complementary strand to the 3' → 5' template can be synthesized continuously and is denoted the leading strand whereas the complement of the 5' → 3' strand must be synthesized in fragments (Okazaki fragments) and is denoted the lagging strand. [7] For the lagging strand, an RNA primer pairs with the template strand which allows for DNA polymerase to generate new complementary DNA that continues to pair with the template. Removal of the RNA primer at the end of the replication process means that the original DNA that the primer is paired with is not duplicated (figure 3). Denoted as the end replication problem, loss of DNA information is an inherent consequence to DNA replication; moreover, continual degradation and loss of information (DNA) results in cell damage and numerous apoptotic pathways. [8] Initially, no information crucial to cellular function is lost due to the fact that the ends of DNA strands contain a non-coding region rich in guanine (G) nucleotides called the telomere. Although this seems like a temporary solution since telomeres will likewise degrade, human telomerase continually extends these regions in cells undergoing significant replication, namely, stem cells, germ cells, and cancer cells. [9]

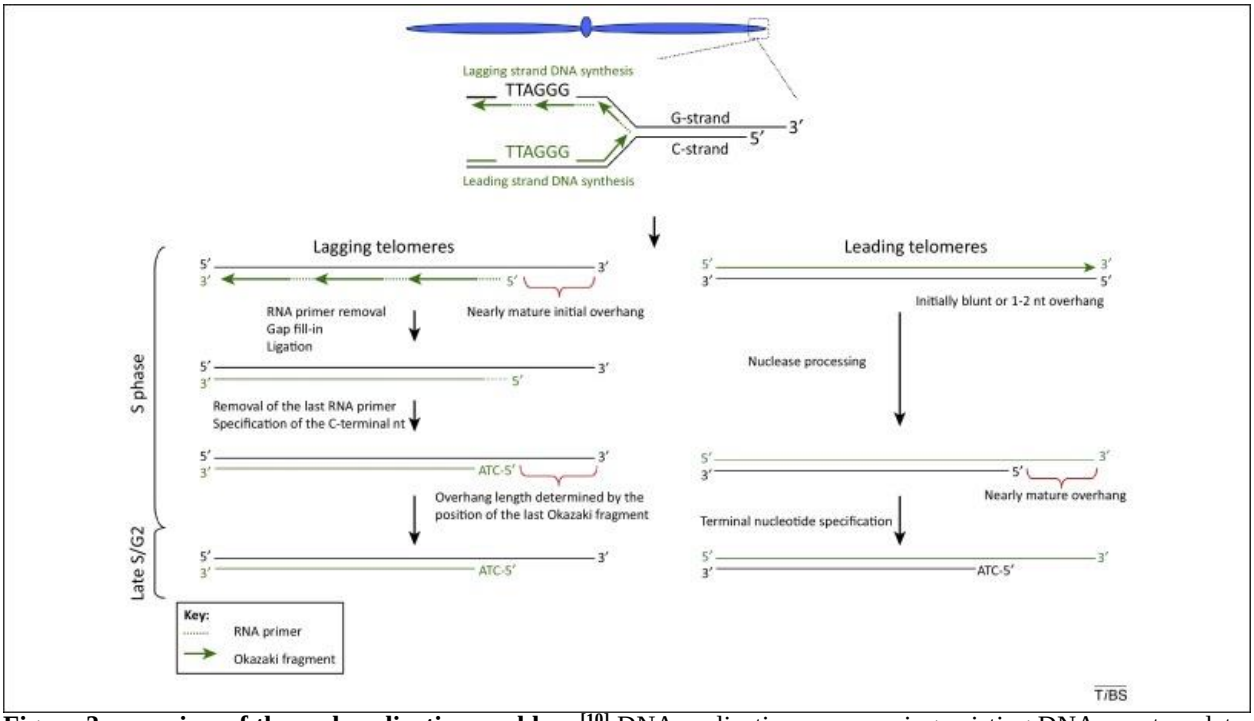

Figure 3: overview of the end replication problem.[10] DNA replication occurs using existing DNA as a template. Replication only occurs in the 5' → 3' direction meaning that there will be a leading and lagging strand: one strand is synthesized in a single iteration, and the other must be generated piece by piece (in the form of Okazaki fragments) as the template strand unwinds, respectively. The unpaired ends are highlighted in red in this figure.

Further investigation of telomerase was achieved through careful observation of the inhibited enzyme complex after exposer to certain small molecules. The isolation of the macrocycle telomestatin **(4)**, from the bacteria *Streptomyces anulatus*, led to some of the first insights into mechanisms of telomerase inhibition. [6] Telomestatin inhibits telomerase rather potently (IC_{50} of 0.2 μM), but failure to inhibit telomerase in a few rare cancer cells sparked a further investigation into the molecule's mode of action. [11] Additional experiments testing the molecules ability to inhibit the reverse transcriptase on the retrovirus HIV [12] revealed that telomestatin had no little to no inhibitory effect on the enzyme. Since telomerase, too, contains a reverse transcriptase, this finding suggested telomestatin acted on a functionality on human telomerase that differed from the reverse transcriptase on HIV. Accumulating evidence pointed to the guanine-rich binding site of telomerase which could inhibit the activity of the molecule by

folding in a G-quadruplex (figure 4). [11, 13] Computational experiments showed that telomestatin stabilized the G-quadruplex *via* a π-π stacking interaction, and this work was supported by the fact that molecules synthesized to more strongly stabilize π-bonding interactions were more potent inhibitors. [14]

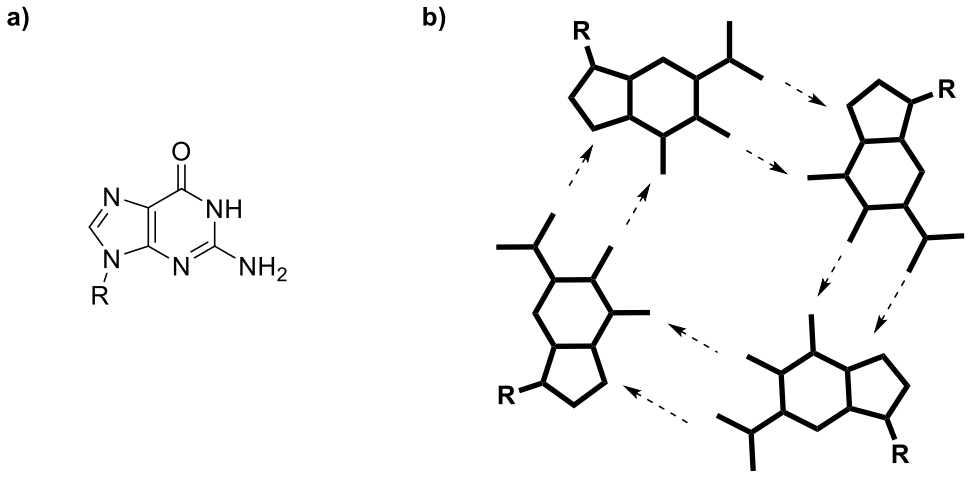

Figure 4: guanine and the G-quadruplex. a) The chemical structure of the guanine base pair on DNA. The R group is representative of the rest of the nucleotide. b) A top-down view of the G-quadruplex, revealing how G residues hydrogen bond to one another and allow nucleotide strands to favorably fold into a stable complex.

Axixnelloside A, like telomestatin, is a potent inhibitor of telomerase, but it likely acts through a different mechanism. Looking at the structures alone, it is clear that the poly-sulfated, lipid-bearing oligosaccharide **(1)** differs significantly from the oxazole-based macrocycle **(4)**. In fact, studies on simpler sulfated saccharides showed that these types of molecules inhibited both telomerase and HIV's reverse transcriptase. [15] Studies on other structurally related compounds further revealed that this inhibition depended heavily on the fatty ester and sulfate moieties since chemical removal of these functional groups invariably lead to severely reduced inhibition ability. [5b, 16] Sulfated telomerase inhibitors like the dictyodendrin A **(2)** lose all inhibitory activity after removal of its sulfate group, and a multitude of fatty acids, specifically oleic acid, were shown to

directly interact with the human telomerase enzyme**.** While these findings suggest that there are other significant means of inhibiting telomerase, the mechanism behind these means are entirely elusive. Thus, axinelloside A presents itself as a privileged molecule that can be used to investigate alternative mechanisms of telomerase inhibition. Because axinelloside A contains sulfate groups and fatty esters, and it strongly inhibits telomerase, it is a choice molecule to modify and use to investigate new inhibition mechanisms.

Oligosaccharides, alone, are difficult molecules to synthesize, and with fatty acyl and anionic sulfate moieties, constructing axinelloside A presents itself as a serious challenge. Closer inspection, however, reveals that the oligosaccharide is primarily composed of alternating galactose and fucose carbohydrate residues along with a *scyllo*-inositol head and an arabinose tail (figure 5). Galactose, fucose, and arabinose are all abundant and fairly cheap carbohydrates, so a synthesis can reasonably start with these molecules to build trimeric and tetrameric oligosaccharides. Undertaking a total synthesis in this fashion (with multiple building blocks) generates less waste and yield more product overall. While a linear total synthesis starts with a single molecule and, by attrition, loses product through subsequent steps, a convergent synthesis limits the product lost through step-wise additions by using more starting materials to combine with synthetic methods. Moreover, because there are so many repeating fucose and galactose residues, the synthesis of a single fucose or galactose building block actually yields five building blocks with minute changes to the protecting groups on the molecule. Multiple dimer, trimer, and tetramer building blocks also inherently generates axinelloside A derivatives that can be used for biological testing: completion of the axinelloside A would yield not only the molecule for testing telomerase inhibition, but a plethora of derivatives that could be modified to test specific aspects of the substrata-enzyme complex.

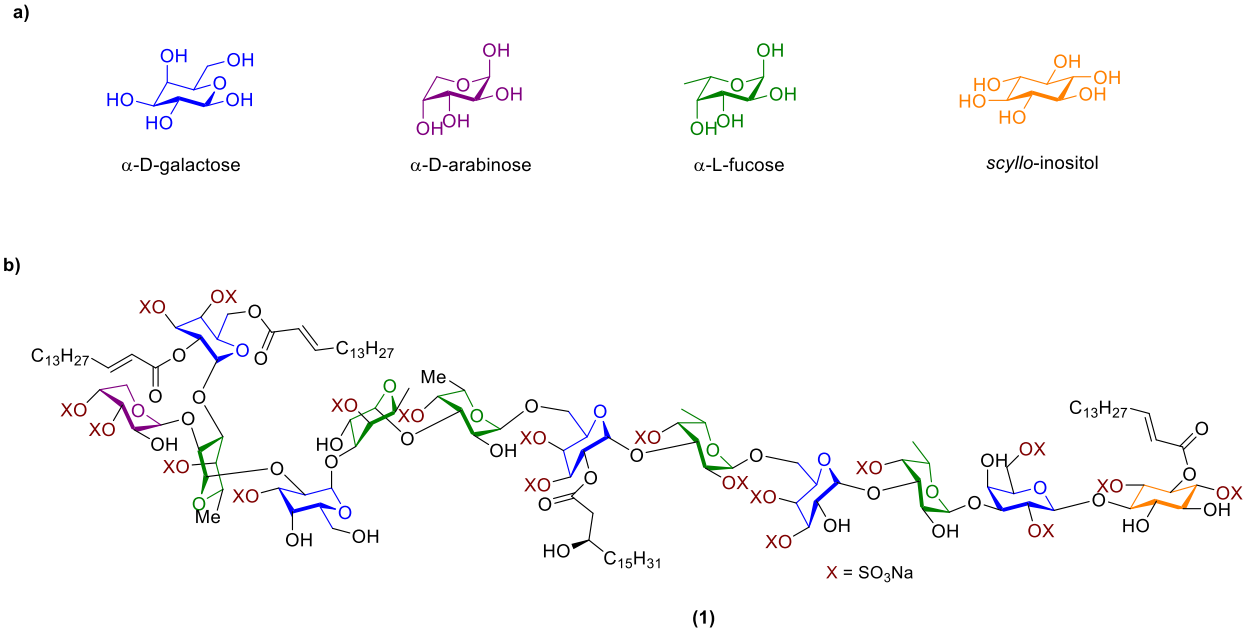

Figure 5: specific residues of axinelloside A. a) Generic, unprotected structure of each carbohydrate constituting axinelloside A and the head of the molecule, *scyllo*-inositol. b) Galactose residues are colored blue, fucose residues are colored green, arabinose is colored purple, and *scyllo*-inositol is colored orange.

The carbocycle at the head of the molecule, *scyllo*-inositol, is a more challenging residue to synthesize. One of the rarer inositol isomers, *scyllo*-inositol contains six equatorial hydroxyl groups which make regioselective modification difficult. Additionally, unlike its more naturally abundant isomer *myo*-inositol (figure 6), the undecorated *scyllo*-inositol is fairly expensive, so a semi-synthesis starting from the pure residue is not an option like galactose, fucose, and arabinose.

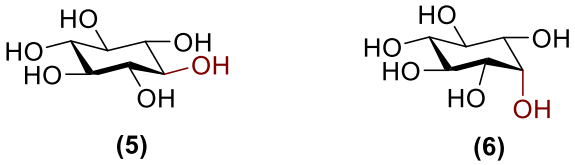

Figure 6: *scyllo*- and *myo* inositol. *Scyllo*-inositol **(5)** and *myo*-inositol **(6)** with the difference in stereochemistry highlighted in red.

1.1.2 *Scyllo*-inositol

Scyllo-inositol, one of many isomers of 1,2,3,4,5,6-cyclohexanehexol, decorates the head of axinelloside A. Unlike the other components of the molecule, *scyllo*-inositol is not a carbohydrate. Although carbohydrates also bear multiple hydroxyl groups, synthesis and modification of carbohydrates are facilitated by the fact that many of the alcohols have unique chemical properties. Not only do carbohydrates contain a highly reactive C6 primary alcohol, but the C1 alcohol (figure 7) is actually part of a hemi-acetal which reduces its nucelophilicity significantly. [17]

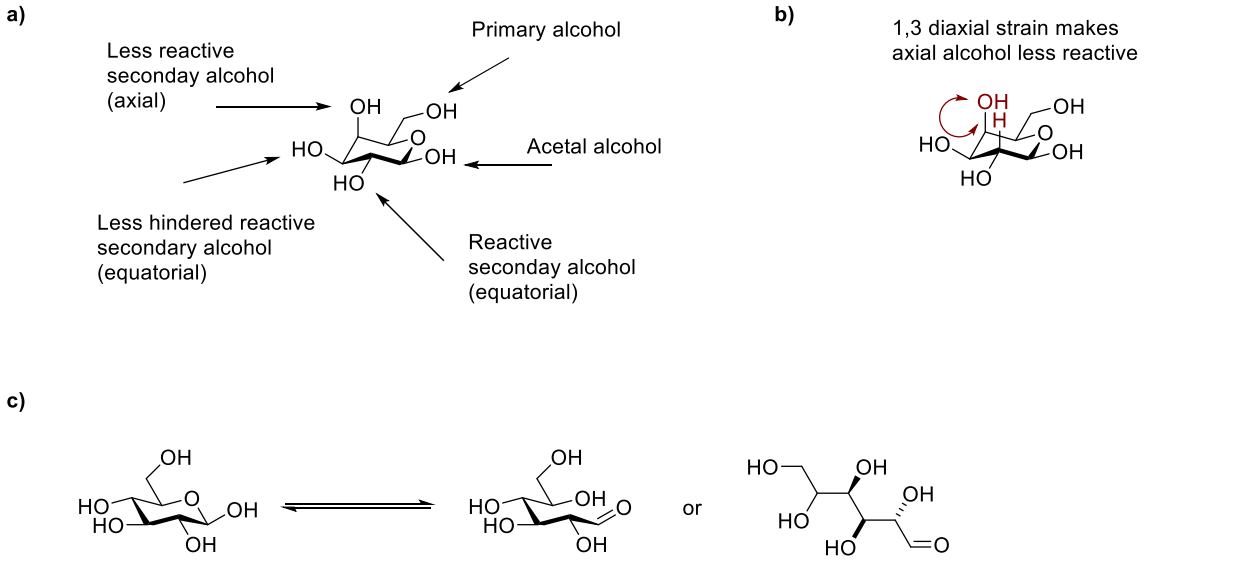

Figure 7: reactivity of alcohols on carbohydrates. a) General explanation of the reactivity of alcohols using galactose as a model carbohydrate. b) Depiction of 1,3 diaxial strain on galactose. c) Equilibrium between cyclic and linear glucose, emphasizing the acetal chemistry of the C1 alcohol.

The remaining alcohols, depending on the specific carbohydrate isomer in question, can also be specifically modified through strategic placement of protecting groups, capitalization on small differences in reactivity between adjacent *cis* and *trans* alcohols (scheme 1). [18]

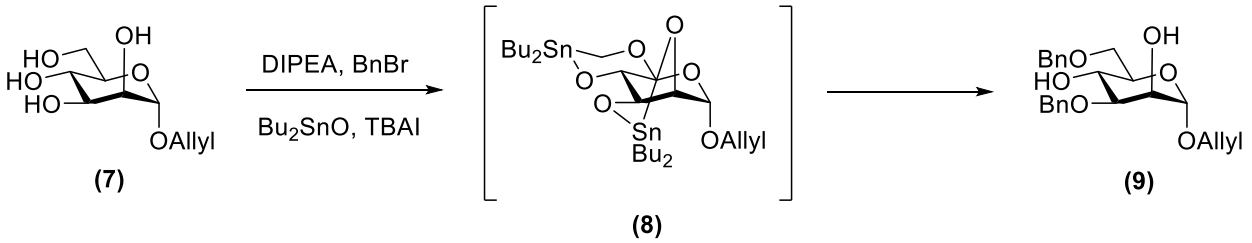

Scheme 1: regioselective benzlyation of mannoside (9). Stannylene acetals like **(8)** exaggerate the slight reactivity difference between the C3 and C4 alcohols. Bonds between oxygen and tin are more nucleophlic due to tin's propensity to donate electron density into the O-Sn σ-bond.

Being comprised of six adjacent alcohols—all secondary and *cis* to one another—*scyllo*-inositol poses a unique synthetic challenge since each hydroxyl group retains the same reactivity as the group adjacent to it. With such similar reactivities, attempts to regioselectively modify one alcohol over another would result in complex mixtures of *scyllo*-inositol regioisomers. Purifying these mixtures would not only be labor-intensive, but isolation would further waste time and resources because most isolated components would be useless since a very specific protection pattern is necessary for the *scyllo*-inositol contained in axinelloside A. This means that a *de novo* synthesis of *scyllo*-inositol is necessary to access an asymmetrically substituted molecule that can be used in the synthesis of axinelloside A.

Although syntheses of *scyllo*-inositol exist, none have been accomplished with multiple different functional groups that allow for regioselective modification. *Myo*-inositol, an epimer of *scyllo*-inositol containing one axial hydroxyl group has been synthesized with useful protecting group strategies. [19] *Myo*-inositol, the most common inositol isomer, is an important modification made to lipooligosaccharides and peptidoglycans that induces specific biological signaling. [20] Because of this, a multitude of synthetic procedures are known to make derivatives of the molecule to probe biological systems. These procedures can thus be capitalized on to generate the asymmetrically protected inositol core which will allow easier access to *scyllo*-

inositol. Once the carbocycle core is established, the use of chemical inversion techniques will grant access to correcting hydroxyl groups that have the wrong stereochemistry (scheme 2).

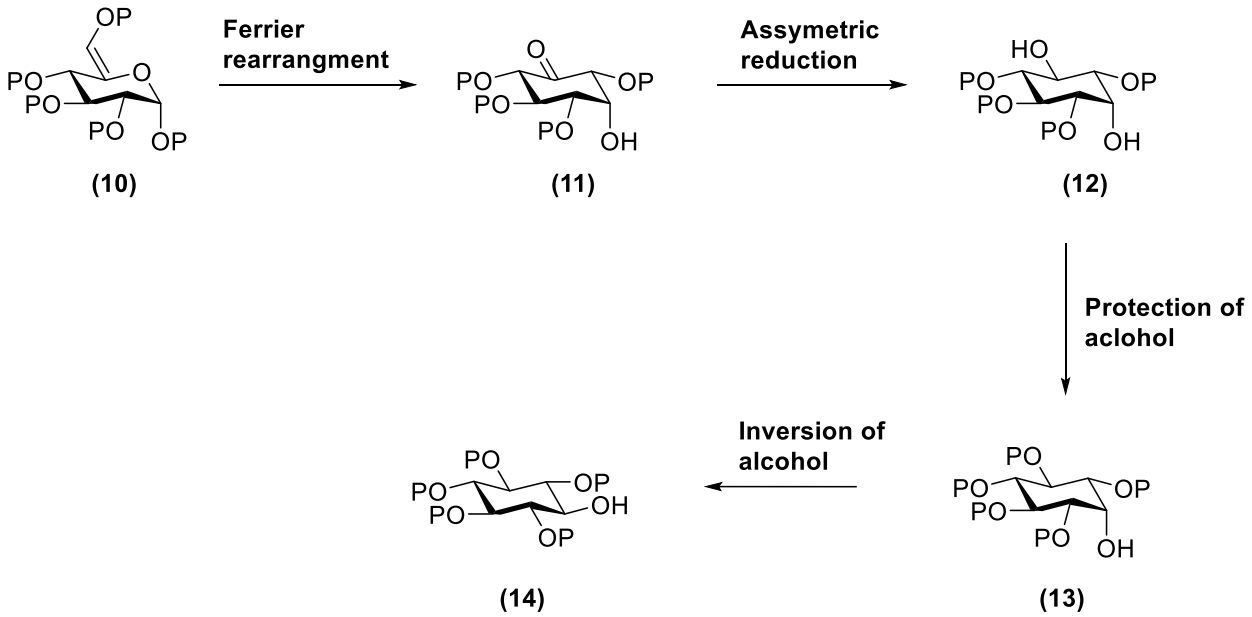

Scheme 2: generalized reaction scheme to make *scyllo*-inositol. P is used to represent a general protecting group. Establishment of the carbocyclic core **(11)** is known *via* a Ferrier II rearrangement on **(10).** From this, an asymmetric reduction followed by a protection and inversion will generate the desired *scyllo*-inositol compound **(14)**.

A reliable method to generate asymmetrically substituted *scyllo*-inositol is not only beneficial for the synthesis of axinelloside A, but for the synthesis of other biologically relevant small molecules as well. Alzheimer, a neurodegenerative disease characterized by neuronal damage incurred from the formation of insoluble amyloid plaques and neurofibrillary tangles, remains a fatal disease without a cure. Although debated, the amyloid β (Aβ) protein that constitutes the majority of the amyloid plaques is believed to cause and signify the neurodegenerative symptoms of Alzheimer disease. Aβ monomers, excised from the surface of neuronal cell membranes by β-secretase, oligomerize facilely and crowd synaptic junctions by which neuron cells transmit messages and cargo. As these oligomers accumulate, neurons malfunction, causing cell death. Additionally, these oligomers possibly cause the formation of

neurofibrillary tangles as tau proteins accumulate in response to increased phosphorylation due to neuronal cell stress and cellular damage caused by Aβ synaptic blockage. [21] This problem, however has shown to be mitigated by *scyllo*-inositol. Multiple studies have shown the molecule's ability to break up and dissociate Aβ plaques, and the molecule had success in treating Alzheimer patients up until a phase II clinical trial where more severe side effects emerged and caused the testing to discontinue. [22] Development of a methodology for the generation of asymmetrically substituted *scyllo*-inositol, however, would grant access to other derivatives with a potential for Alzheimer treatment (figure 8). Despite the initial phase II setback, development of *scyllo*-inositol can continue in an attempt to fight the deleterious Aβ plaques.

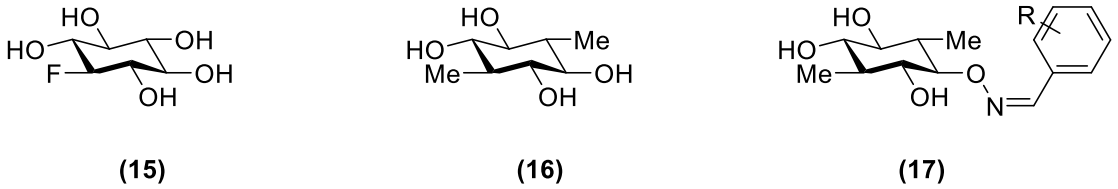

(15) **(16)** **(17)**

Figure 8: biologically relevant *scyllo*-inositol derivatives. 1-Deoxy-1-fluoro-*scyllo*-inositol **(15)**. [23] 1,4-dideoxy-1,4-dimethyl-*scyllo*-inositol **(16)**. [24] Oxime derivatives of **(16)**, **(17).** [25]

1.2 RESULTS AND DISCUSSION

1.2.1 Synthesis of asymmetrically substituted *scyllo*-inositol

Beginning with commercially available α-D-methyl-glucopyranoside **(18)**, large quantities of **(19)** were prepared *via* a protection with *p*-anisaldehyde (scheme 3). Anisaldehyde dimethyl acetal was generated *in situ* using methyl orthoformate before the addition of **(18)** and a catalytic amount of *p*-toluenesulfonic acid. The establishment of this benzylidine moiety protected the C6 and C4 hydroxyl groups, generating a bicyclic ring structure which could be asymmetrically cleaved later. The remaining C2 and C3 hydroxyl groups were protected with benzyl either moieties in basic conditions using benzyl bromide (BnBr) and a polar, aprotic solvent to facilitate the reaction (DMF). In order to cleave the benzylidene ring at the C6 position, BH_3, in the presence of Bu_2BOTf, was used, yielding **(21)** with a free C6 hydroxyl group and the C4 hydroxyl group protected by a *p*-methoxybenzyl group. This BH_3 mediated reaction worked to generate the C6 alcohol exclusively, and this reaction was carried out on a multi-gram scale without any erosion of regioselectivity. With the free primary alcohol in hand, a Swern oxidation was undertaken to generate the corresponding aldehyde followed immediately by conversion to the enol acetate **(22)** with exclusively *Z* diastereoselectivity.

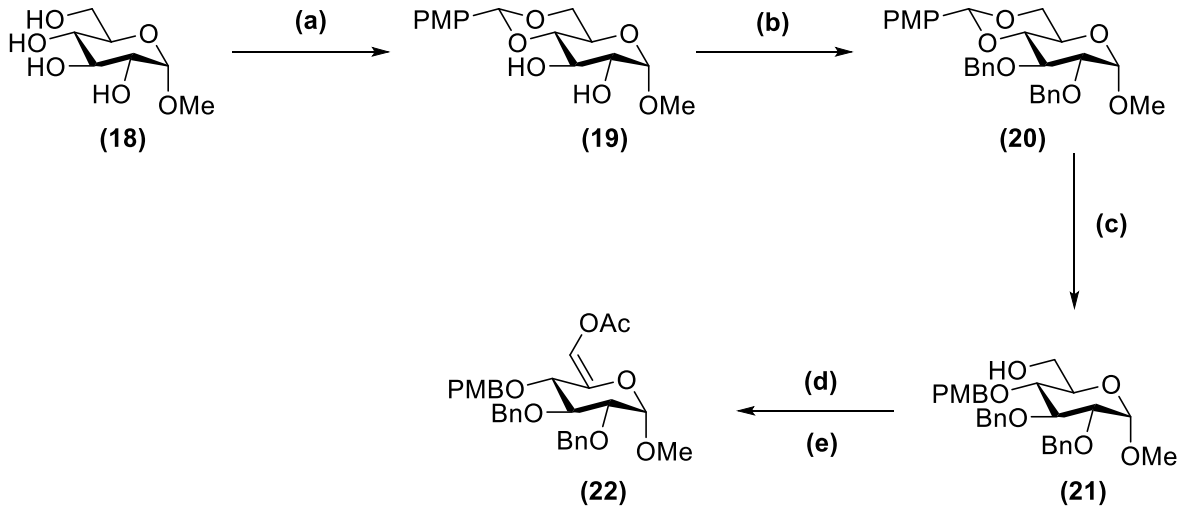

Scheme 3: generation of the enol acetate (22). Reagents and conditions: (a) p-anisaldehyde (1.0 equiv), p-TsOH (0.025 equiv), $(MeO)_3CH$ (1.2 equiv), DMF, 50 °C, 82%; (b) BnBr (3.0 equiv), NaH (10 equiv), KHMDS (0.5 equiv), DMF, rt, 73%; (c) BH_3–THF (10 equiv), *n*-Bu_2BOTf (1.95 equiv), 0 °C, 70%; (d) $(COCl)_2$ (1.2 equiv), DMSO (2.5 equiv), Et_3N (3.5 equiv), CH_2Cl_2, -78 to -40 °C; (e) Ac_2O (12 equiv), K_2CO_3 (8 equiv), MeCN, reflux, 61% (over 2 steps).

With significant quantities of enol acetate **(22)** in hand, we were posed to explore the feasibility of using the Ferrier rearrangement (Ferrier II reaction [26]) to generate the general inositol carbocyclic scaffold (scheme 4). The Ferrier rearrangement capitalizes on a carbohydrate's ability to undergo enol chemistry in the presence of a promoter (scheme 5). Mercury (II) salts promote this reaction by activating the enol ether so that the olefin undergoes hydroxymercuration, generating ketal **(27)**. This ketal can then trigger an opening of the pyranoside, and a following intramolecular enol addition to the resulting aldehyde, which forms a C-C bond, would close the ring again to form the carbocycle.

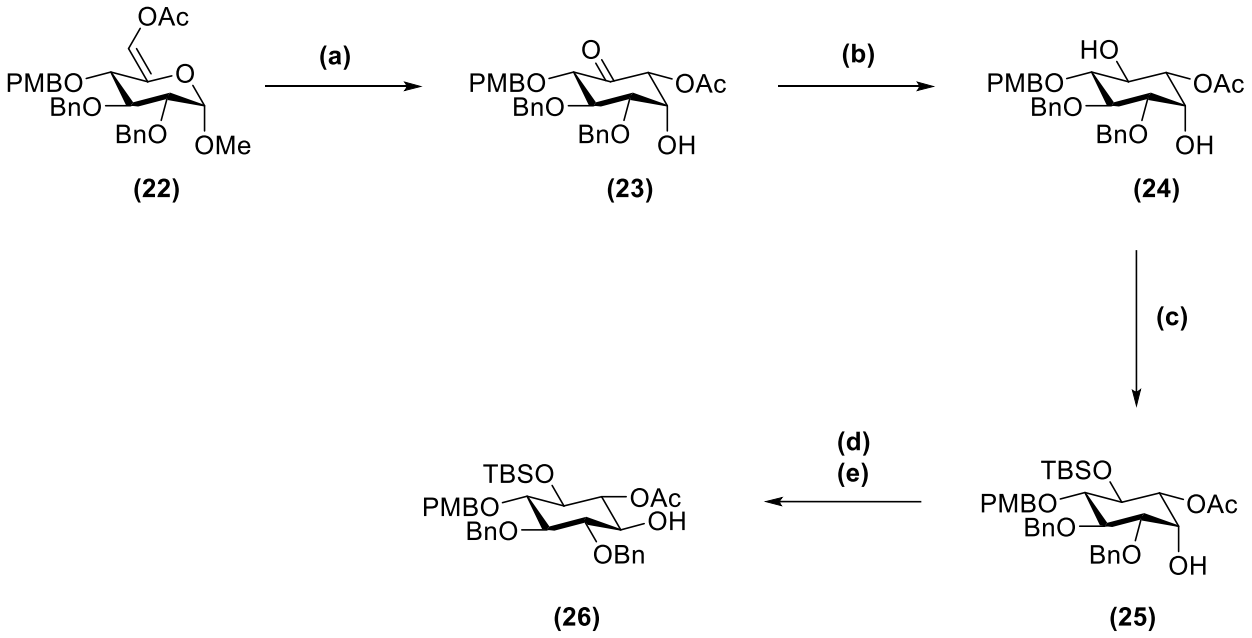

Scheme 4: generation of asymmetrically substituted *scyllo*-inositol (26). Reagents and conditions: (a) $Hg(TFA)_2$ (1.2 equiv), H_2O/AcONa, rt, 50%, (b) $NaBH(OAc)_3$ (10 equiv), AcOH (16 equiv), MeCN, rt, 82%; (c) TBSOTf (1.5 equiv), 2,6-lutidine (2 equiv), CH_2Cl_2, rt, 34%; (d) $(COCl)_2$ (1.2 equiv), DMSO (2.5 equiv), Et_3N (3.5 equiv), CH_2Cl_2, -78 to -40 °C; (e) $NaBH_4$ (4.5 equiv), MeOH, rt, 39% (over 2 steps).

Rearrangement of **(22)** using mercuric chloride generated the anticipated *myo*-inositol product albeit in poor (35%) yield. [cite] Absolute configuration of this product was assured using NMR spectroscopy. The two adjacent C1 and C6 protons coupled with a *J* value between 2.5 and 3.0 Hz (^{1}HNMR: 4.31 ppm, t, ^3J = 2.8 Hz) indicating a *cis* relationship. A more Lewis acidic mercury (II) salt source ($Hg(TFA)_2$), however, provided a much more reasonable (50%) yield along with the generation of some (7%) of the C1 epimer.

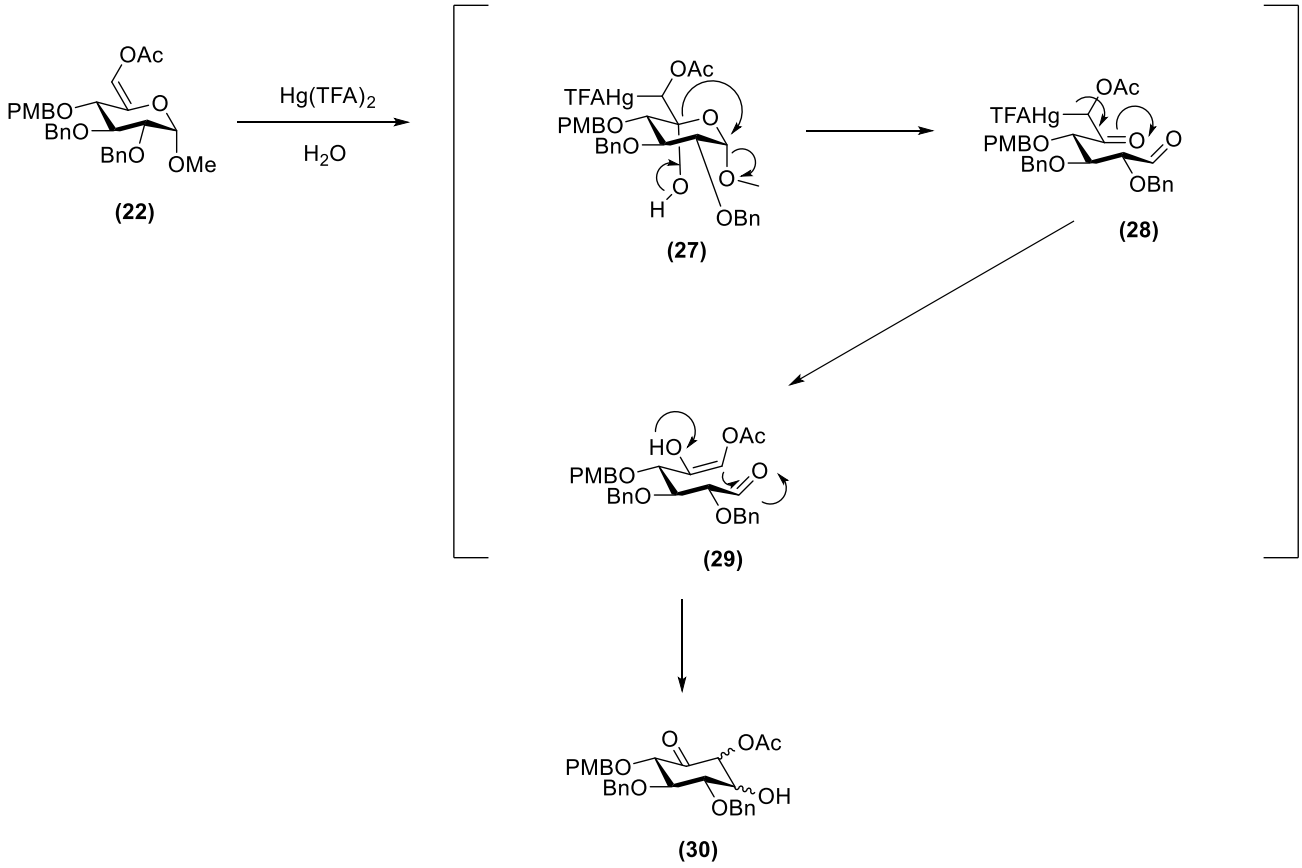

Scheme 5: generalized mechanism of the Ferrier II reaction. This Ferrier II reaction (Ferrier carbocyclization) was promoted using $Hg(TFA)_2$ salt in the presence of water. The mercury salt induced a hydroxymercuration which poised **(22)** to open and then close *via* an intramolecular enol attack on the aldehyde. Absolute configuration is intentionally left vague since four theoretical stereoisomers can be generated from this reaction.

Although four stereoisomers can be formed from the Ferrier rearrangement, **(23)** was the major isomer. This stereoselectivity can be understood as a consequence of the molecule's preferred conformation in three-dimensional space in addition to the molecular orbital overlap that would result in a reaction (figure 9). Because the formation of the enol acetate **(29)** is reversible, the thermodynamically stable *trans* (*E*) isomer **(32)** would be preferred over the more sterically congested *cis* (*Z*) isomer **(31)**. When situated in a chair-like configuration, it is clear that the *E* isomer would generate a down-facing, equatorial acetoxy moiety, which is consistent with the experimental evidence. To further support this, careful purification and isolation of the products

of the Ferrier reaction yielded no isomer where the acetoxy moiety was situated in an axial configuration. The predominance of the axial hydroxyl group over the equatorial group, though, is more unexpected. Because axial substituents experience more 1,3 diaxial strain, they are less likely to form in a reaction since they require more energy. [27] Considerations of proper molecular orbital overlap and the electronics of the molecule account for this energy barrier, and provide a justification for the preference of the axial diastereomer. The conformations presented in b) (figure 6) depict more realistic bond angle with regards to the enol. The highest occupied molecular orbital in this system—the nucleophile—is the enol system where electron density primarily resides on the oxygen and carbon (figure 6: c)). The lowest occupied molecular orbital—the electrophile—(LUMO) of this system is the π -π^* antibonding orbital. When the HOMO interacts with the LUMO, a C-C bond will form that closes the ring, and the C-O double bond will break, leaving only the C-O σ bond. When the aldehyde points up, the orbitals from the HOMO are nearly perpendicular with the LUMO orbitals. This poor overlap would make orbital interaction and thus the reaction slow, generating little of the up-facing, equatorial alcohol. The downwards-facing aldehyde, however, allows much better orbital overlap, resulting in the reaction favoring this conformation which generates the axial hydroxyl group. Poor overlap does not make the reaction impossible; rather, it slows the reaction down. This is why both the axial and equatorial hydroxyl epimer were found with the axial, and much more of the axial product is formed.

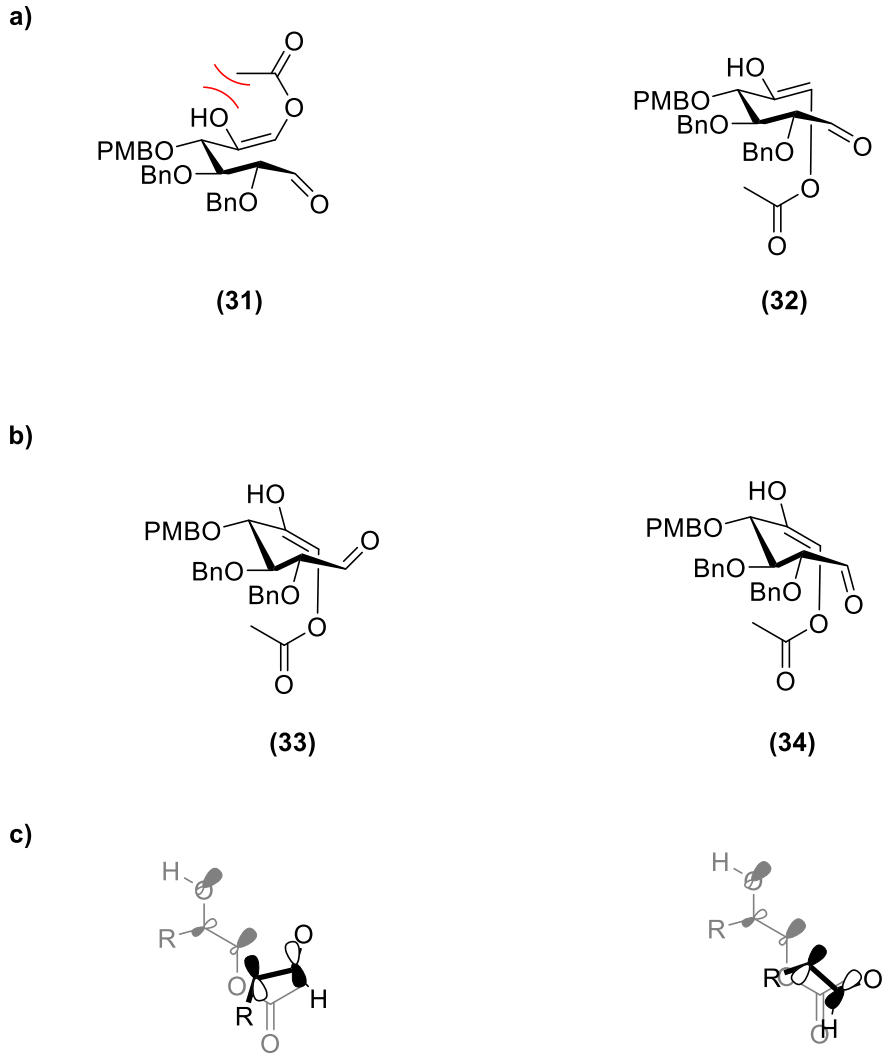

Figure 9: conformational consideration of intermediate (29). a) Two conformers of **(29)** in a distorted chair conformation. Unlike the (*E*) isomer **(32),** the (*Z*) isomer **(31)** is subject to unfavorable steric clash marked in red. b) Drawn more realistically to account for the bond angles of enol **(32)**, conformer **(34)** shows more direct orbital overlap than **(33).** c) Molecular structure is simplified to emphasize the directionality of the enol HOMO with the aldehyde's antibonding LUMO. The left diagram is representative of **(33)**, and the right diagram is representative of **(34)**.

Reduction of the C5 ketone proceeded smoothly using $NaBH_4$ affording **(24)** as a single isomer, *trans* to the C6 acetoxy moiety (^{1}HNMR: 4.11 ppm, t, ^3J = 9.8 Hz). This selectivity is believed to occur due to the axial C1 hydroxyl group acting as a directing group for the incoming hydride nucleophile. The resulting diol **(24)** posed an initial challenge due to the fact that both secondary alcohols maintained similar reactivity. This minor difference arises from the fact that

one alcohol (C1) is in an axial position and the other (C5) is in an equatorial position. When constrained to a six-member ring, axial functional groups encounter more 1,3 diaxial strain with other axial protons than equatorial function groups, and as a result, are less reactive. First, a silylation of the equatorial hydroxyl group was attempted using TBSOTf and 2,6-lutidine at -78 °C, but this resulted in a mixture of **(25)** and the doubly protected product in a 1.4: 1 ratio. At an elevated temperature (0 °C), the reaction proceeded more smoothly generating **(25)** in moderate (39%) yields without a double silylation. The remainder of the material failed to react. Affirmation of the silylation on the equatorial hydroxyl group was achieved using long range ^{29}Si-^{1}H HMBC experiments. This experiment shows correlations between proton and silicon atoms over the range of two to three bonds, which means that only the protons on the methyl and *tert*-butyl group on the silicon in addition to the proton attached to the same carbon atom as the protected alcohol would generate a signal. Because this signal was only seen on the proton by the equatorial hydroxyl group and not the alcohol, the reaction was deemed regioselective and successful (figure 10).

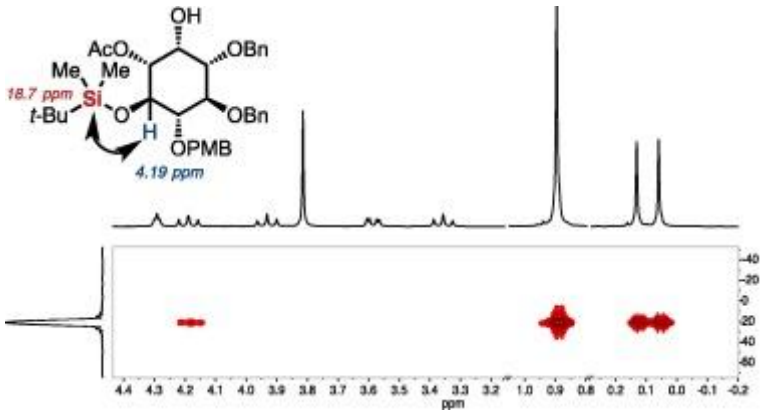

Figure 10: ^{29}Si-^{1}H HMBC correlation spectrum. [28] The horizontal axis shows the ^{1}H NMR spectrum for the molecule, and the vertical axis shows the ^{29}Si NMR spectrum. Areas marked in red are where a correlation between a specific proton and silicon atom occur. This can be seen as three clusters: 1) a red cluster occurs at 0.70 ppm, showing the correlation of the protons on the two methyl groups attached to the silicon; 2) a red cluster occurs at 0.89 ppm, showing the correlation of the protons on the *tert*-butyl group attached to the silicon; 3) a red cluster occurs at 4.19 ppm—the chemical shift of the highlighted proton—showing the correlation of this hydrogen atom with the silicon. There are no other correlations, suggesting that the silyl protection only occurred on this alcohol.

With the asymmetrically substituted *myo*-inositol **(25)**, only one transformation remained: the inversion of the C1 hydroxyl group to form the *scyllo*-inositol stereoisomer. Typically, an inversion of a single alcohol can be reliably accomplished using Mitsunobu reaction conditions (tri-substituted phosphine, an azodicarboxylate source, and a weak nucleophile, typically a carboxylic acid). The Mitsunobu reaction works primarily to turn an alcohol into a good leaving group as the oxygen-carbon bond is irreversibly cleaved to form a very stable phosphine oxide (P-O double bond). [29] In order to achieve this, an azodicarboxylate is stirred in the presence of the phosphine and the acid, activating both (scheme 6). The alcohol is then added to react with the activated phosphine which forms the phosphonium complex that behaves as a good leaving group during an S_N2 reaction by the activated acid.

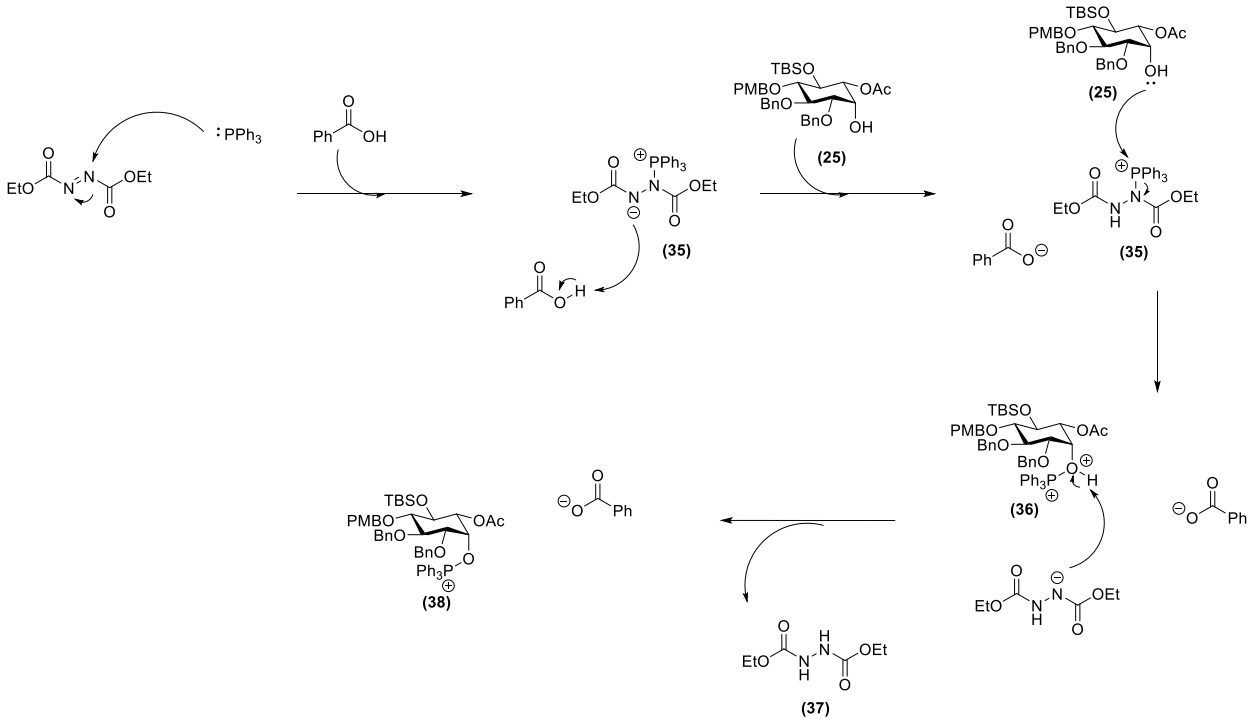

Scheme 6: mechanism of the Mitsunobu reaction. An arrow-pushing mechanism of the Mitsunobu reaction is presented using PPh_3, DEAD, BzOH, and **(25)**. The mechanism only includes steps up to intermediate **(38).** The consequences of the multiple final steps are considered more closely in scheme 7.

This reaction was attempted on **(25)** using PPh_3, diethyl azodicarboxylate (DEAD), and BzOH as the carboxylic acid source at room temperature. Initially, the starting material was not consumed, so a more reactive phosphine ((2,2-bis(diphenylphosphino)ethane) was used in the place of PPh_3. It was assumed that the bulky and highly congested nature of **(25)** made reaction with the activated phosphonium slow, so a more reactive and less sterically hindered phosphine would ideally facilitate the reaction. The new reaction conditions failed to generate any product; however, after extensive heating some conversion of the starting material was observed. Unfortunately, purification and characterization of the product revealed that the wrong diastereomer **(40)** was formed, and the reaction carried out with a retention of stereochemistry (scheme 7). Because there was no inversion, the benzoate must not have displaced the activated hydroxyl group, and instead the alcohol was activated, generating the phosphonium intermediate, but the molecule was too sterically congested for an S_N2 displacement on the carbon center. This would force the benzoate nucleophile to react with the more available phosphonium electrophilic center, cleaving the hydroxyl P-O bond in the process. The activated benzoate could then undergo a nucleophilic substitution as the hydroxyl group from the inositol species attacks the activated carbonyl center and displaces the benzoate oxygen, causing it to leave as a phosphine oxide. This would result in a retention of stereochemistry, which is the only product isolated from the Mitsunobu reaction on **(40)**.

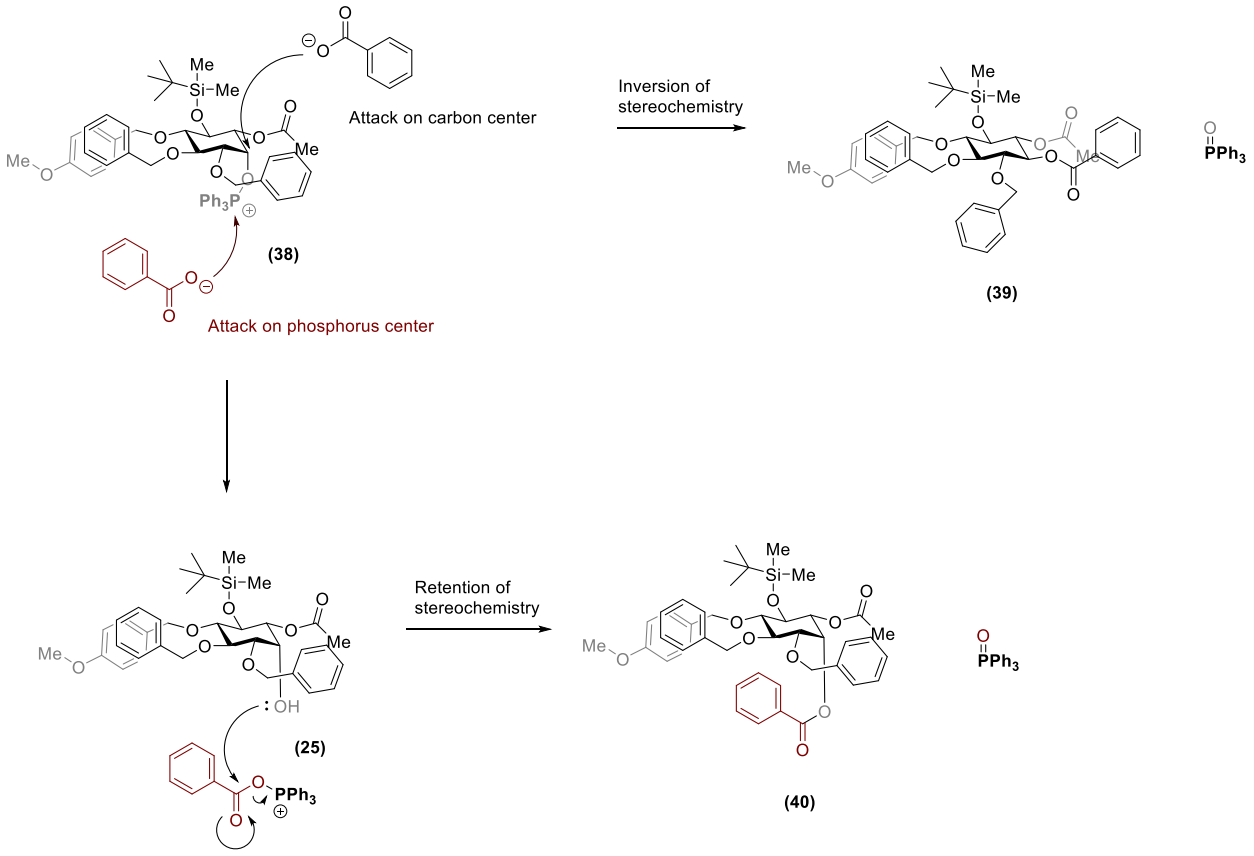

Scheme 7: stereochemical consequences of benzoate attack on intermediate (38). The consequences of the benzoate ion attacking either the electrophilic carbon or the electrophilic phosphonium. An attack on the carbon center would result in an inversion of stereochemistry, but an attack on the phosphonium center would result in a reaction pathway leading to a retention of stereochemistry. Atoms and bonds that are behind other atoms and bonds are highlighted in gray for clarity. The retention pathway is depicted using a red benzoate ion.

Seeing that a one-step inversion of the C1 position would be problematic, an alternative approach was attempted using a two-step oxidation–reduction sequence. Oxidation of the C1 hydroxyl group would result in a ketone that contains neither axial nor equatorial stereochemistry, essentially resetting the stereocenter. A subsequent reduction of this ketone would reestablish the stereocenter, albeit not very selectively. Thus, the hydroxyl group in **(25)** was oxidized under the Swern conditions and the resultant ketone was reduced with $NaBH(OAc)_3$ in AcOH, providing **(26)** in 58% yield. As expected, the hydroxyl group was generated in a mixture of the axial and equatorial diastereomer there was a mixture of equatorial and axial ((diastereometic ratio: 1.5:1.0). The more reactive and smaller reducing reagent, $NaBH_4$, provided *scyllo*-inositol in a better yield (62%) and

higher diastereoselectivity (1.7:1.0). The configuration of the product was assured using the same spectroscopic methods as were used earlier (^{1}H NMR spectroscopy), which revealed the diagnostic coupling constant of the C1 proton (t, 3 J = 9.6 Hz). This indicated that the newly formed alcohol had an equatorial configuration. Although this method generates a mixture of stereoisomers, this mixture is exclusively the product and starting material. After chromatographic purification, the product **(26)** along with the starting material **(25)** were both recovered, meaning that the same reaction could be performed again to enrich the amount of equatorial alcohol available since more of the equatorial diastereomer is generated than the axial. The moderate selectivity achieved can be rationalized by a participatory effect of the acetoxy moiety. The down-facing acetoxy group likely played a minor role in aiding the delivery of the hydride from the bottom face, which would preferentially generate scyllo-inositol.

1.3 CONCLUSIONS

This work describes the total synthesis and characterization of an asymmetrically substituted *scyllo*-inositol. Starting from a cheap an abundant α-D-methylglucoside, generation of the product **(26)** was achieved in nine steps. This synthesis capitalized on a Ferrier II reaction which generated the inositol core, followed by a selective reduction, protection, and stereochemical inversion to convert the initial *myo*-inositol to the desired *scyllo*-inositol. This asymmetric *scyllo*-inositol will be used in the future as the head of axinelloside A (figure 11). Moreover, this molecule is the most challenging building block of axinelloside A, and with its completion, only simple carbohydrate building blocks remain. This asymmetric *scyllo*-inositol will be used in the future as the head of axinelloside A.

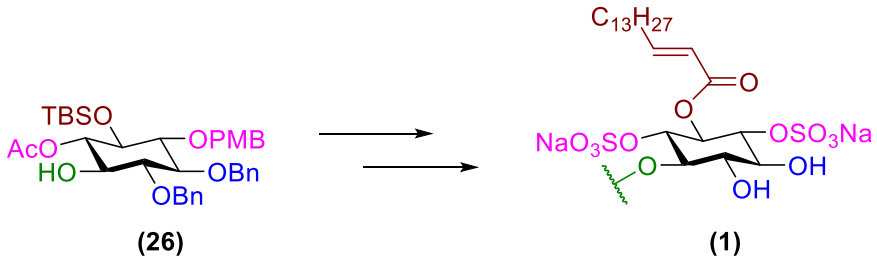

Figure 11: colored depiction of asymmetric *scyllo*-inositol. The different protecting groups will be selectively removed to regioselectively establish the bonds that constitute the correct decorations for the *scyllo*-inositol in axinelloside A.

2.0 EXPERIMENTAL SECTION

General procedure

All chemicals were purchased as reagent grade and used without further purification, unless otherwise noted. Solvents were filtered through a column of activated alumina prior to use. All reactions were carried out under dry N_2 in oven-dried glassware. TLC analyses were performed on Merck TLC plates and visualizations were performed with UV light and/or Hanessian stain. Column chromatography was performed on silica gel (230-400 mesh). Melting points were recorded in open capillaries and uncorrected. ^{1}H and ^{13}C NMR spectra were recorded on Bruker 300/ Varian 400/ Varian 500 MHz instruments are reported as follows: chemical shift (δ), multiplicity (s = singlet, d = doublet, t = triplet, q = quartet, br = broad, m = multiplet), coupling constants (Hz), and integration. The residual solvent reference peaks were used from published literature.[1] 2D NMR experiments were performed using standard parameters (*200 and More NMR Experiments*, S. Berger, S. Braun, Wiley-VCH, **2004**). IR measurements were performed on Agilent Cary 630 FT/IR instrument and optical rotations were measured on JASCO P-1030.

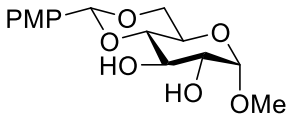

(19)

Methyl 4,6-*O*-[(*R*)-(4-methoxyphenyl)methylene]-α-D-glucopyranoside (7). To a solution of methyl α-D-glucopyranoside (2.14 g, 11.0 mmol) in dry (10.0 mL), *p*-anisaldehyde (1.36 g, 10.0 mmol), and *p*-toluenesulfonic acid (0.0476 g, 0.250 mmol) were added and stirred for 5 min at rt

under a nitrogen atmosphere. Methyl orthoformate (1.31 mL, 12.00 mmol) was added dropwise and the resulting solution was stirred for 15 min at rt. Afterwards, the solution was subject to rotary evaporation in a 50 °C water bath where the reaction was monitored by TLC until completion. After the reaction is completed, the mixture was diluted with EtOAc (50 mL), and the resulting solution was quenched with saturated aqueous $NaHCO_3$ (150 mL). The aqueous layer was washed with EtOAc (3 x 75 mL), and the combined organic layers are washed with brine, dried over Na_2SO_4, and concentrated. The resulting crude product was stirred with hexanes (200 mL) for 16 h and the heterogeneous solutions was filtered to provide the insoluble material, which was rinsed. The organic solvent was evaporated to afford **7** (2.82 g, 82%) as a white powder. The analytical data match previous report by Chen *et al.* (*Org. Lett.* **2005**, *7*, 3343).

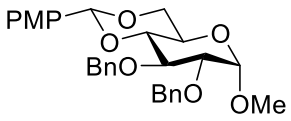

(20)

Methyl-2,3-bis-*O*-benzyl-4,6-*O*-[(*R*)-(4-methoxyphenyl)methylene]-*α*-D-glucopyranoside (8). A solution of **7** (13.9 g, 44.5 mmol) in dry DMF (200 mL) was cooled to 0 °C before and benzyl bromide (15.9 mL, 134 mmol) was added followed by NaH (17.8 g, 445 mmol, 60% dispersion in mineral oil) and a solution of KHMDS (44.5 mL, 22.3 mmol, 0.5 M in PhMe). The reaction was stirred at rt for 14 h, quenched with sat. NH_4Cl (200 mL), and the aqueous layer was extracted with Et_2O (2 x 150 mL). The combined organic layers were dried (Na_2SO_4) and concentrated. The crude material was purified by flash column chromatography (Hexanes/EtOAc, 5:1) to afford **C**

(16.0 g, 73%) as a white powder: $[\alpha]_D^{24}$: -35.5 (c 0.66, $CHCl_3$); IR (ATR) ν = 3050, 2933, 2824, 1644, 1511, 1389, 1240 cm^{-1}; ^1H NMR: (300 MHz, Chloroform-*d*) δ 7.53 – 7.29 (m, 12H), 7.01 – 6.85 (m, 2H), 5.54 (s, 1H), 5.02 – 4.82 (m, 3H), 4.73 (d, *J* = 12.2 Hz, 1H), 4.63 (d, *J* = 3.7 Hz, 1H), 4.28 (dd, *J* = 9.9, 4.6 Hz, 1H), 4.07 (t, *J* = 9.2 Hz, 1H), 3.84 (s, 3H), 3.79 – 3.54 (m, 4H), 3.43 (s, 3H).; ^{13}C NMR (75 MHz, Chloroform-*d*) δ 160.0, 138.8, 138.2, 130.0, 128.5, 128.3, 128.1, 128.0, 127.9, 127.6, 127.4, 113.6, 101.3, 99.3, 82.1, 79.2, 78.6, 75.3, 73.8, 69.0, 62.4, 55.3; MS (ESI): *m/z* calcd. for $C_{29}H_{35}O_7Na$ $[M+Na]^+$: 515.2, found: 515.2.

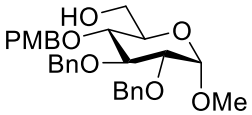

(21)

Methyl 2,3-bis-*O*-benzyl-4-*O*-[(4-methoxyphenyl)methyl]-α-D-glucopyranoside (9). Neat **8** (1.00 g, 2.03 mmol) was transferred into a dry flask, and the flask was purged with nitrogen, cooled to -20 °C, and a solution of BH_3·THF (20.3 mL, 20.3 mmol, 1 M in THF) was added. The resulting solution was stirred for 15 min, the reaction mixture was warmed up to 0 ºC and a solution of *n*-Bu_2BOTf (3.96 mL, 3.96 mmol, 1 M in CH_2Cl_2) was added dropwise. The reaction mixture was stirred at 0 ºC for 4 hours, quenched with Et_3N (2.0 mL) and MeOH (20 mL). The mixture was then stirred for additional 30 min, concentrated, and passed through a block of silica. The filtrate was concentrated, and the crude oil was purified by flash chromatography (Hexanes/EtOAc, 70:30) to yield **9** (0.699 g, 70%) as a clear oil: $[\alpha]_D^{24}$: +8.8 (c 0.10., $CHCl_3$); IR (neat) ν = 3451, 2919, 1620, 1533, 1432, 1376, 1221 cm^{-1}; ^1H NMR (300 MHz, Chloroform-*d*) δ 7.48 – 7.31 (m,

10H), 7.26 – 7.20 (m, 2H), 6.93 – 6.83 (m, 2H), 5.01 (d, *J* = 11.0 Hz, 1H), 4.89 (s, 1H), 4.88 – 4.81 (m, 1H), 4.81 (d, *J* = 2.9 Hz, 1H), 4.68 (d, *J* = 12.1 Hz, 1H), 4.60 (d, *J* = 6.4 Hz, 1H), 4.57 (s, 1H), 4.01 (dd, *J* = 9.6, 8.8 Hz, 1H), 3.81 (s, 3H), 3.63-3.76 (m, 3H), 3.57 – 3.48 (m, 2H), 3.38 (s, 3H).; ^{13}C NMR (75 MHz, Chloroform-*d*) δ 160.0, 138.8, 138.2, 130.0, 128.5, 128.3, 128.1, 128.0, 127.9, 127.6, 127.4, 113.6, 101.3, 99.3, 82.1, 79.2, 78.6, 75.3, 73.8, 69.0, 62.4, 55.3; MS (ESI): *m/z* calcd. for $C_{29}H_{34}O_7Na$ $[M+Na]^+$: 517.2, found: 517.2.

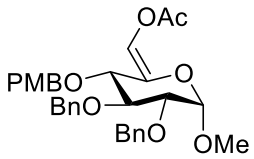

(22)

Methyl 6-*O*-acetyl-2,3-bis-*O*-(phenylmethyl)-4-*O*-[(4-methoxyphenyl)methyl]-α-D-gluco-5-enpyranoside (10). Under a nitrogen atmosphere, oxalyl chloride (0.152 mL, 1.77 mmol) was dissolved in dry DCM (8.0 mL) and dry DMSO (0.251 mL, 3.54 mmol) was added dropwise via syringe at -78 °C. The reaction mixture was stirred at -78 °C for 15 min and a solution of **9** (700 mg, 1.42 mmol) in dry DCM (4.0 mL) was added and stirred for 15 min followed by freshly distilled Et_3N (0.99 mL, 7.80 mmol). The reaction was allowed to warm up to – 40 °C, stirred at this temperature for 1 h, poured into a separatory funnel containing hexanes (100 mL) and water. The organic layer was washed with 0.5 M sodium bisulfate solution (3 x 50 mL), 1.0 M pH 7 phosphate buffer (50 mL), dried with Na_2SO_4, and concentrated. The crude residue was then immediately dissolved in dry MeCN (15 mL). Ac_2O (1.61 mL, 17.0 mmol) and anhydrous K_2CO_3 (1.57 g, 11.3 mmol) were added, and the reaction mixture was refluxed for 4 h. Once all of the

aldehyde was consumed, the reaction was transferred into a vigorously stirring mixture of 0.2 M pH 7 phosphate buffer (50 mL) and hexanes/EtOAc mixture (1:1, 50 mL) and allowed to stir for 30 min. The layers were separated and the organic layer was washed with 1.0 M pH7 phosphate buffer (50 mL), dried (Na_2SO_4), and concentrated. Purification by flash column chromatography on SiO_2 (Hexanes/EtOAc, 85:15) afforded **10** (0.0461 g, 61%) as a clear oil: $[\alpha]_D^{25}$: -53.7 (c 1.0., $CHCl_3$); IR (ATR) ν = 2946, 1755, 1605, 1522, 1431, 1390 cm^{-1}; ^1H NMR (300 MHz, Chloroform-*d*) δ 7.41 – 7.28 (m, 12H), 7.20 (d, *J* = 1.5 Hz, 1H), 4.92 (d, *J* = 10.9 Hz, 1H), 4.89 – 4.82 (m, 2H), 4.75 – 4.72 (m, 1H), 4.72 – 4.65 (m, 3H), 4.02 – 3.95 (m, 2H), 3.82 (s, 0H), 3.67 – 3.57 (m, 3H), 3.50 (s, 3H), 2.18 (s, 3H).; ^{13}C NMR (75 MHz, Chloroform-*d*) δ 167.3, 159.4, 138.6, 138.0, 135.1, 129.7, 128.5, 128.4, 128.1, 128.0 (2), 127.7, 123.1, 113.9, 99.8, 81.3, 79.1, 75.7, 74.2, 73.7, 56.2, 55.3, 20.6; MS (ESI): *m/z* calcd. for $C_{31}H_{34}O_8H$ $[M+H]^+$: 535.2, found 535.2.

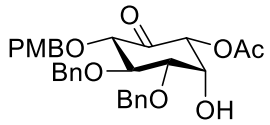

(23)

(2R, 3S, 4S, 5R, 6S)-2-Acetoxy-3-hydroxy-4,5-bis-*O*-benzyl-6-*O*-[(4-methoxyphenyl)methyl] -cyclohexanone (11). A solution of **10** (450 mg, 0.842 mmol) in a 4:1 mixture of acetone (8 mL) and water (2 mL) was cooled to 0 °C and $Hg(TFA)_2$ (431 mg, 1.01 mmol) was added. The reaction mixture was stirred at rt for 15 minutes, 3.0 M solution of NaOAc (0.3 mL) was added, followed by brine (0.9 mL). The mixture was stirred at rt for 4 h, poured into a separatory funnel containing a 1:1 hexanes/EtOAc mixture (50 mL) and water (25 mL). The organic layer was washed with

water (30 mL) and 1.0 M pH 7 phosphate buffer, dried (Na_2SO_4), concentrated. Purification by flash column chromatography on SiO_2 (Hexanes/EtOAc, 70:30) afforded **11** (0.221 g, 50%) as an off-white amorphous solid: $[\alpha]_D^{25}$: -2.4 (c 1.0., $CHCl_3$); IR (ATR) ν = 3477, 3472, 2926, 2360, 1762, 1615, 1522, 1451, 1399, 1223 cm^{-1}; ^1H NMR (300 MHz, Chloroform-*d*) δ 7.42 – 7.32 (m, 10H), 7.28 – 7.23 (m, 2H), 6.90 – 6.84 (m, 2H), 4.98 – 4.83 (m, 3H), 4.75 (dd, *J* = 10.3, 2.7 Hz, 1H), 4.72 – 4.67 (m, 3H), 4.31 (t, *J* = 2.8 Hz, 1H), 4.10 (t, *J* = 9.8 Hz, 1H), 3.94 (t, *J* = 9.5 Hz, 1H), 3.81 (s, 3H), 3.58 (dd, *J* = 9.5, 2.7 Hz, 1H), 3.38 (t, *J* = 9.4 Hz, 1H), 2.45 (s, 1H), 2.24 (s, 1H), 2.18 (s, 3H); ^{13}C NMR (75 MHz, Chloroform-*d*) δ 170.7, 159.4, 138.5, 137.4, 129.7, 128.6, 128.4, 128.1, 127.9, 127.7, 114.0, 82.5, 80.9, 80.1, 75.8, 75.3, 73.0, 72.9, 70.3, 67.8, 55.3, 21.1; MS (ESI) *m/z* calcd. for $C_{30}H_{32}O_8Na$ $[M+Na]^+$: 543.2, found 543.2.

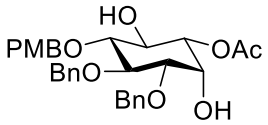

(24)

l-*O*-Acetyl-3,4-bis-*O*-benzyl-5-*O*-[(4-methoxyphenyl)methyl]-D-*myo*-inositol (12). Under a nitrogen atmosphere, **11** (230 mg, 0.442 mmol) was dissolved dry MeCN (55 mL), and $NaBH(OAc)_3$ (0.437 g, 4.42 mmol) was added followed by AcOH (0.411 mL, 7.21 mmol). The reaction was stirred at rt for 1 h, poured into a separatory funnel containing 0.5 M solution of $Na_2S_2O_3$ (20 mL) and EtOAc (80 mL). The phases were separated and the organic layer was washed with 0.5 M solution of $Na_2S_2O_3$ (2 x 30 mL), 2.0 M pH 7 phosphate solution (2 x 30mL), dried (Na_2SO_4), and concentrated. Purification by chromatography on SiO_2 (Hexanes/EtOAc,

60:40) provided **12** (0.191 g, 82%) as an off-white amorphous solid: $[\alpha]_D^{24}$: -1.7 (c 1.0., $CHCl_3$); IR (ATR) ν = 3491, 3425, 3019, 2984, 1724, 1615, 1520, 1452, 1382, 1216 cm^{-1}; ^1H NMR (500 MHz, Chloroform-*d*) δ 7.40 – 7.30 (m, 10H), 7.29 – 7.24 (m, 2H), 6.90 – 6.85 (m, 2H), 4.98 – 4.84 (m, 3H), 4.75 (dd, *J* = 10.3, 2.8 Hz, 1H), 4.72 – 4.67 (m, 3H), 4.30 (t, *J* = 2.8 Hz, 1H), 4.11 (t, *J* = 9.8 Hz, 1H), 3.94 (t, *J* = 9.5 Hz, 1H), 3.81 (s, 3H), 3.58 (dd, *J* = 9.5, 2.7 Hz, 1H), 3.38 (t, *J* = 9.4 Hz, 1H), 2.53 (s, 1H), 2.33 (s, 1H), 2.18 (s, 3H);); ^{13}C NMR (101 MHz, Chloroform-*d*) δ 170.8, 159.4, 138.5, 137.4, 130.4, 129.7, 128.6, 128.4, 128.1, 127.9, 127.7, 114.0, 82.5, 80.9, 80.1, 75.8, 75.3, 73.0, 72.8, 70.2, 67.7, 55.3, 21.1; MS (ESI) *m/z* calcd. for $C_{30}H_{34}O_8Na$ $[M+Na]^+$: 545.2, found: 545.2.

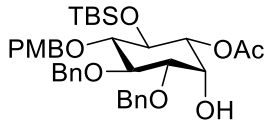

(25)

l-*O*-Acetyl-3,4-bis-*O*-benzyl-5-*O*-[(4-methoxyphenyl)methyl]-6-*O*-*tert*-butyldimethylsilyl-D-*myo*-inositol (13). To a solution of **12** (0.165 g, 0.316 mmol) in dry CH_2Cl_2 (3.0 mL), 2,6-lutidine (0.0820 mL, 0.632 mmol) was added followed by TBSOTf (0.0970 mL, 0.474 mmol). The resulting solution is allowed to stir at rt for 4 h, the reaction mixture was quenched with sat. NH_4Cl (1 mL), extracted with DCM (3 x 3 mL), and the combined organic layers were washed with sat. $CuSO_4$ (5 mL), dried (Na_2SO_4), and concentrated. Purification by chromatography on SiO_2 (Hexanes/EtOAc, 85:15) provided **13** (0.0680 g, 34%) as a clear oil: $[\alpha]_D^{24}$: -28.8 (c 1.0., $CHCl_3$); IR (ATR) ν = 3481, 2938, 2933, 2839, 2374, 1755, 1621, 1523, 1359, 1222 cm^{-1}; ^1H NMR (300

MHz, Chloroform-*d*) δ 7.40 – 7.20 (m, 12H), 6.91 – 6.79 (m, 2H), 4.99 – 4.65 (m, 7H), 4.29 (t, *J* = 2.7 Hz, 1H), 4.19 (dd, *J* = 9.9, 8.9 Hz, 1H), 3.93 (t, *J* = 9.5 Hz, 1H), 3.81 (s, 3H), 3.59 (dd, *J* = 9.6, 2.7 Hz, 1H), 3.36 (t, *J* = 9.2 Hz, 1H), 2.42 (s, 1H), 2.18 (s, 3H), 0.90 (s, 9H), 0.13 (s, 3H), 0.06 (s, 3H); ^{13}C NMR (101 MHz, Chloroform-*d*) δ 165.8, 154.0, 133.8, 132.7, 126.1, 123.9, 123.8, 123.5, 123.3, 123.1, 123.0, 122.8, 108.8, 78.4, 76.5, 75.3, 71.0, 70.6, 69.5, 68.0, 66.1, 62.9, 50.4, 21.0, 16.7, 13.2; MS (ESI) *m/z* calcd. for $C_{36}H_{48}O_8SiNa$: 659.3 $[M+Na]^+$, found 659.3.

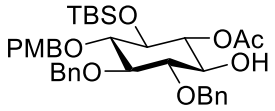

(26)

l-*O*-Acetyl-3,4-bis-*O*-benzyl-5-*O*-[(4-methoxyphenyl)methyl]- 6-*O*-*tert*-butyldimethylsilyl-D-*scyllo*-inositol (14). Under a nitrogen atmosphere, oxalyl chloride (1.43 µL, 0.0167 mmol) was dissolved in dry CH_2Cl_2 (0.25 mL), cooled to -78 °C, and dry DMSO (2.4 µL, 0.0332 mmol) was added. The reaction mixture was allowed to stir at this temperature for 30 min, and a solution of **13** (9.0 mg, 0.0153 mmol) in dry DCM (0.25 mL) was added. The mixture was stirred for 1 h 15 min, and freshly distilled Et_3N (9.3 µL, 0.0665 mmol) was added. The reaction mixture was allowed to warm up to -40 °C over 1 h, transferred to a separatory funnel containing 1 mL of sat. NH_4Cl, and the aqueous layer was extracted with CH_2Cl_2 (3x 2 mL). The combined organic layers were dried (Na_2SO_4), concentrated, and the resultant oil was immediately placed under nitrogen and dissolved in dry MeOH (0.5 mL). $NaBH_4$ (2.9 mg, 0.077 mmol) was added, and the reaction was stirred at rt for 1 h, poured into a separatory funnel containing sat. NH_4Cl (1.0 mL),

and the aqueous layer was extracted with CH_2Cl_2 (3 x 2.0 mL). The combined organic layers were dried (Na_2SO_4), concentrated, and purified by prep-TLC on SiO_2 (CH_2Cl_2/methanol, 100:1) to provide **14** (3.5 mg, 39%) as a white solid: $[\alpha]_D^{24}$: -20.8 (c 1.0., $CHCl_3$); IR (ATR) ν = 3405, 2919, 2833, 1744, 1623, 1521, 1438, 1377, 1224 cm^{-1}; ^1H NMR (500 MHz, Chloroform-*d*) δ 7.28 (s, 12H), 6.83 (d, *J* = 8.7 Hz, 1H), 4.97 – 4.84 (m, 5H), 4.77 (d, *J* = 8.1 Hz, 1H), 4.75 (d, *J* = 8.4 Hz, 1H), 3.81 (s, 3H), 3.68 (t, *J* = 9.2 Hz, 1H), 3.56 – 3.41 (m, 5H), 2.14 (s, 3H), 0.87 (s, 9H), 0.08 (d, *J* = 3.2 Hz, 3H), 0.02 (s, 3H).; ^{13}C NMR (126 MHz, Chloroform-*d*) δ 79.2, 78.9 (2), 70.3, 68.8, 68.5, 51.2; MS (ESI) *m/z* calcd. for $C_{36}H_{48}O_8SiNa$ $[M+Na]^+$: 659.3 found 659.3.

BIBLIOGRAPHY

[1] K. Warabi, T. Hamada, Y. Nakao, S. Matsunaga, H. Hirota, R. W. van Soest, N. Fusetani, *Journal of the American Chemical Society* **2005**, *127*, 13262-13270.

[2] D. J. Newman, G. M. Cragg, *Journal of natural products* **2007**, *70*, 461-477.

[3] P. J. Scheuer, *Science* **1990**, *248*, 173-177.

[4] K. A. Houck, R. J. Kavlock, *Toxicology and applied pharmacology* **2008**, *227*, 163-178.

[5] aE. Delfourne, F. Darro, N. Bontemps-Subielos, C. Decaestecker, J. Bastide, A. Frydman, R. Kiss, *Journal of medicinal chemistry* **2001**, *44*, 3275-3282; bK. Warabi, S. Matsunaga, R. W. van Soest, N. Fusetani, *The Journal of organic chemistry* **2003**, *68*, 2765-2770; cJ. W. Blunt, B. R. Copp, W.-P. Hu, M. Munro, P. T. Northcote, M. R. Prinsep, *Natural product reports* **2009**, *26*, 170-244.

[6] K. Shin-ya, K. Wierzba, K.-i. Matsuo, T. Ohtani, Y. Yamada, K. Furihata, Y. Hayakawa, H. Seto, *Journal of the American Chemical Society* **2001**, *123*, 1262-1263.

[7] H. J. Kriegstein, D. S. Hogness, *Proceedings of the National Academy of Sciences* **1974**, *71*, 135-139.

[8] M. Z. Levy, R. C. Allsopp, A. B. Futcher, C. W. Greider, C. B. Harley, *Journal of molecular biology* **1992**, *225*, 951-960.

[9] T. R. Cech, J. Lingner, in *Ciba Foundation Symposium 211-Telomeres and Telomerase*, Wiley Online Library, **1997**, pp. 20-40.

[10] P. Martínez, M. A. Blasco, *Trends in biochemical sciences* **2015**, *40*, 504-515.

[11] M.-Y. Kim, H. Vankayalapati, K. Shin-Ya, K. Wierzba, L. H. Hurley, *Journal of the American Chemical Society* **2002**, *124*, 2098-2099.

[12] R. Esnouf, J. Ren, C. Ross, Y. Jones, D. Stammers, D. Stuart, *Nature Structural and Molecular Biology* **1995**, *2*, 303.

[13] aL. Guittat, A. De Cian, F. Rosu, V. Gabelica, E. De Pauw, E. Delfourne, J.-L. Mergny, *Biochimica et Biophysica Acta (BBA)-General Subjects* **2005**, *1724*, 375-384; bT. Doi, K. Shibata, M. Yoshida, M. Takagi, M. Tera, K. Nagasawa, K. Shin-ya, T. Takahashi, *Organic & biomolecular chemistry* **2011**, *9*, 387-393.

[14] M. Tera, H. Ishizuka, M. Takagi, M. Suganuma, K. Shin-ya, K. Nagasawa, *Angewandte Chemie International Edition* **2008**, *47*, 5557-5560.

[15] T. Eitsuka, K. Nakagawa, M. Igarashi, T. Miyazawa, *Cancer letters* **2004**, *212*, 15-20.

[16] M. Oda, T. Ueno, N. Kasai, H. Takahashi, H. Yoshida, F. Sugawara, K. Sakaguchi, H. Hayashi, Y. Mizushina, *Biochemical Journal* **2002**, *367*, 329.

[17] J. M. Sugihara, in *Advances in carbohydrate chemistry*, *Vol. 8*, Elsevier, **1953**, pp. 1-44.

[18] aM. Giordano, A. Iadonisi, *The Journal of organic chemistry* **2013**, *79*, 213-222; bS. David, S. Hanessian, *Tetrahedron* **1985**, *41*, 643-663.

[19] D. C. Billington, *Chemical Society Reviews* **1989**, *18*, 83-122.

[20] G. E. Gillaspy, *New Phytologist* **2011**, *192*, 823-839.

[21] aI. Benilova, E. Karran, B. De Strooper, *Nature neuroscience* **2012**, *15*, 349; bD.-S. Wang, D. W. Dickson, J. S. Malter, *International journal of clinical and experimental pathology* **2008**, *1*, 5.

[22] M. P. Thomas, S. J. Mills, B. V. Potter, *Angewandte Chemie International Edition* **2016**, *55*, 1614-1650.

[23] F. McPhee, C. Downes, G. Lowe, *Biochemical Journal* **1991**, *277*, 407.

[24] C. A. Hawkes, L. H. Deng, J. E. Shaw, M. Nitz, J. McLaurin, *European Journal of Neuroscience* **2010**, *31*, 203-213.

[25] J. Shaw, J. Chio, S. Dasgupta, A. Lai, G. Mo, F. Pang, L. Thomason, A. Yang, C. Yip, M. Nitz, *ACS chemical neuroscience* **2012**, *3*, 167-177.

[26] N. Chida, T. Sato, *The Chemical Record* **2014**, *14*, 592-605.

[27] K. S. Pitzer, W. E. Donath, in *Molecular Structure And Statistical Thermodynamics: Selected Papers of Kenneth S Pitzer*, World Scientific, **1993**, pp. 98-103.

[28] J. Rodriguez, M. A. Walczak, *Tetrahedron Letters* **2016**, *57*, 3281-3283.

[29] T. Y. S. But, P. H. Toy, *Chemistry–An Asian Journal* **2007**, *2*, 1340-1355.